



HAL
open science

IL versus DES: Impact on chitin pretreatment to afford high quality and highly functionalizable chitosan

Gael Huet, Caroline Hadad, Jose M. Gonzalez-Dominguez, Matthieu Courty, Arash Jamali, Dominique Cailleu, Albert Nguyen van Nhien

► To cite this version:

Gael Huet, Caroline Hadad, Jose M. Gonzalez-Dominguez, Matthieu Courty, Arash Jamali, et al.. IL versus DES: Impact on chitin pretreatment to afford high quality and highly functionalizable chitosan. Carbohydrate Polymers, 2021, 269, 10.1016/j.carbpol.2021.118332 . hal-03612247

HAL Id: hal-03612247

<https://u-picardie.hal.science/hal-03612247>

Submitted on 2 Aug 2023

HAL is a multi-disciplinary open access archive for the deposit and dissemination of scientific research documents, whether they are published or not. The documents may come from teaching and research institutions in France or abroad, or from public or private research centers.

L'archive ouverte pluridisciplinaire **HAL**, est destinée au dépôt et à la diffusion de documents scientifiques de niveau recherche, publiés ou non, émanant des établissements d'enseignement et de recherche français ou étrangers, des laboratoires publics ou privés.



Distributed under a Creative Commons Attribution - NonCommercial 4.0 International License

1 **IL versus DES: Impact on chitin pretreatment to afford** 2 **high quality and highly functionalizable chitosan**

3

4 Gaël Huet,^a Caroline Hadad,^a Jose M. González-Domínguez,^b Matthieu Courty,^c Arash
5 Jamali,^d Dominique Cailleu^e and Albert Nguyen van Nhien^{*a}

6

7 ^a Laboratoire de Glycochimie, des Antimicrobiens et des Agroressources, UMR CNRS 7378,
8 Université de Picardie Jules Verne, 33 rue Saint Leu - UFR des Sciences – 80039 Amiens cedex,
9 France.

10 ^b Group of Carbon Nanostructures and Nanotechnology, Instituto de Carboquímica (ICB-CSIC),
11 C/Miguel Luesma Castán 4, 50018 Zaragoza (Spain).

12 ^c Laboratoire de Réactivité et Chimie des Solides, UMR CNRS 7314, Université de Picardie Jules
13 Verne, HUB de l’Energie, 33 rue Saint Leu - 80039 Amiens Cedex, France.

14 ^d Plateforme de Microscopie Electronique – Université de Picardie Jules Verne, HUB de l’Energie, 33
15 rue Saint Leu - 80039 Amiens Cedex, France.

16 ^e Plateforme analytique, Université de Picardie Jules Verne, UFR des Sciences Bâtiment Serres-
17 Transfert Rue Dallery - Passage du sourire d’Avril 80039 AMIENS Cedex 1, France.

18 *E-mail : albert.nguyen-van-nhien@u-picardie.fr

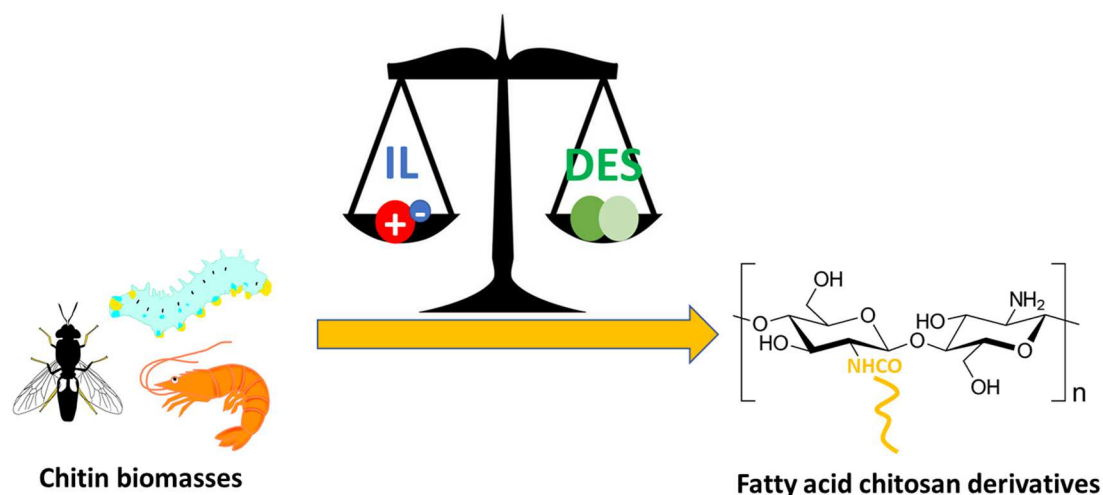
19

20 **ABSTRACT**

21 Chitin is mainly extracted from crustaceans, but this resource is seasonally dependent and can
22 represent a major drawback to satisfy the traceability criterion for high valuable applications. Insect
23 resources are valuable alternatives due to their lower mineral content. However, the deacetylation of
24 chitin into chitosan is still an expensive process. Therefore, we herein compare the impact of both
25 DES/IL-pretreatments on the efficiency of the chemical deacetylation of chitin carried out over two
26 insect sources (*Bombyx eri*, BE and *Hermetia illucens*, HI) and shrimp shells (S). The results showed
27 that chitosans obtained from IL-pretreated chitins from BE larva, present lower acetylation degrees
28 (13-17%) than DES-pretreated samples (18-27%). A selective *N*-acylation reaction with oleic acid has
29 also been performed on the purest and most deacetylated chitosans leading to high substitution degrees
30 (up to 27%). The overall approach validates the proper chitin source and processing methodology to
31 achieve high quality and highly functionalizable chitosan.

32

33 **GRAPHICAL ABSTRACT**



34

35 **KEYWORDS**

36 Chitin, chitosan, room temperature ionic liquid, deep eutectic solvent, functionalization, fatty acid.

37

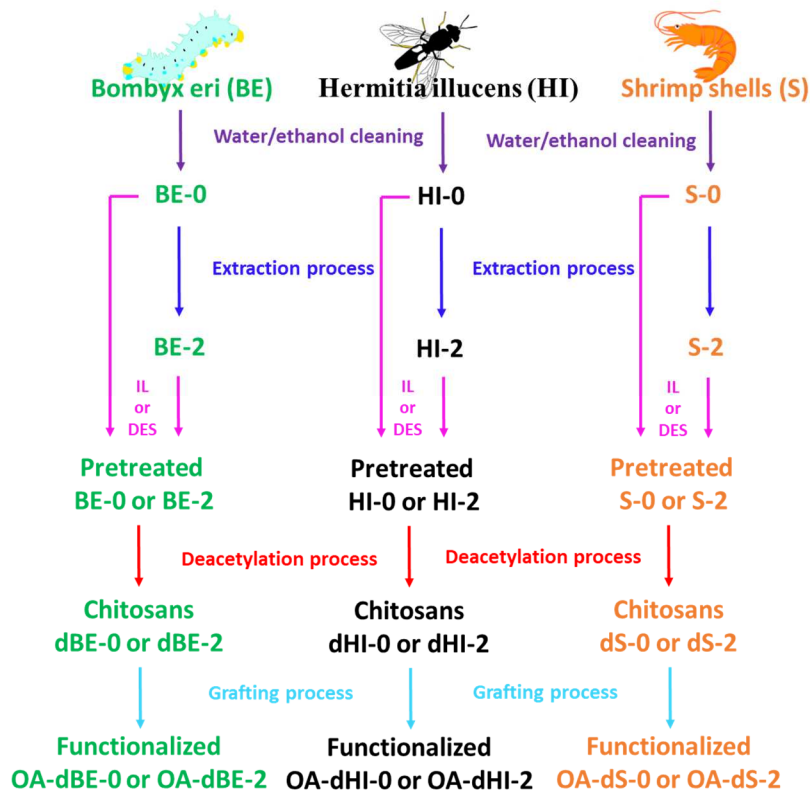
38 **INTRODUCTION**

39 Chitosan, a biopolysaccharide composed of glucosamine units linked together by β -1,4
 40 bonding, is usually produced by deacetylation of chitin, which is mainly extracted from crustacean
 41 shells, insect cuticles or other microorganisms such as bacteria, fungus and mycetes (Hamed, Özogul,
 42 and Regenstein 2016). Both, chitin and chitosan, are biocompatible, biodegradable and non-toxic. In
 43 addition to being soluble in acidic media, chitosan also presents versatile biological activity and has
 44 gained considerable interests for biomedical applications. Indeed, thanks to its antimicrobial activity
 45 and good antioxidant properties, its wound healing properties can prevent infection, allowing good
 46 oxygen permeation (Altiok, Altiok, and Tihminlioglu 2010). Chitosan is also a promising biopolymer
 47 for drug delivery systems to treat diseases such as cancer, optical diseases, and colon diseases (Pan et
 48 al. 2002, Elgadir et al. 2015). Another field of application is related to the use of modified chitosan in
 49 fuel cells. Modified chitosan could represent an environmentally friendlier and economically better
 50 alternative to the currently used polymer electrolytes in hydrogen fuel cell (Ma and Sahai 2013). The
 51 adsorption/biosorption process for the removal or recovery of heavy metal ions and/or radionuclides
 52 from wastewater using naturally occurring chitosan, modified chitosan and chitosan composites have
 53 also been widely reported (Wang and Chen 2014). Even if those properties are well known and
 54 promising in various scientific fields, some drawbacks stand against its development: (i) the extraction
 55 and purification of chitin is costly and environmentally burdening due to the huge amount of waste
 56 water produced during both processes (Khanafari, Marandi, and Sanathei 2008); (ii) chemical
 57 treatments used to obtain chitosan from chitin adversely affect the physical and chemical properties of
 58 these biopolymers (Gadgey and Bahekar 2017, Bajaj, Winter, and Gallert 2011); and (iii) the use of
 59 chitosan in its original form is a limitation for many applications (i. e. poor solubility at physiological
 60 pH, low mechanical strength) and modifications are needed.

61 Due to its generally high crystallinity index, chemical deacetylation of chitin through
62 concentrated alkali treatment has a low success rate to obtain a highly deacetylated chitosan in only
63 one cycle of reaction. Therefore, the reaction must be repeated several times, significantly increasing
64 the cost and the polluting nature of this process as well as entailing a molecular weight heterogeneity.
65 To overcome these issues, Aspra et al. proposed the use of chitin deacetylase as a greener method to
66 perform the deacetylation reaction (Aspras, Jaworska, and Górak 2017). However, the efficiency of
67 the process depends on chitin solubility to obtain a high molecular weight chitosan as the solubility
68 decreases strongly for high molecular weight chitin and the chitin deacetylase might stop working.
69 Mechanical treatments such as grinding or ultrasonication in the presence of NaOH are efficient
70 techniques to obtain low molecular weight chitosan with short reaction times and low acetylation
71 degrees but with low yields and concomitant depolymerization during the reaction (Anwar, Anggraeni,
72 and Amin 2017). The authors also studied the maceration technique, which can be an option to redress
73 the low yields but it needs longer reaction times for the deacetylation step. Recently, the work of Di
74 Nardo et al. has demonstrated that the maceration technique combined with ball milling leads to
75 chitosan with a high degree of deacetylating and high molecular weight (Di Nardo et al. 2019).
76 However, this deacetylation technique is costly in terms of time.

77 In a recent work, we have demonstrated that chitin extracted from *Bombyx eri* (BE) insect
78 larvae can be a very good alternative for the chitin production, as this insect's cuticle contains less
79 minerals and possesses a lower degree of crystallinity than the commercial shrimp source (Huet et al.
80 2020). We also demonstrated that an ionic liquid (IL) pretreatment on insect chitin at different purity
81 degrees enhanced its digestibility by chitinase, leading to high yields of mono and chito-oligomers
82 compared to shrimp shells (Husson et al. 2017). In addition, ionic liquids such as 1-ethyl-3-methyl
83 imidazolium [C₂mim][OAc] was not only able to solubilize chitin by disrupting the hydrogen bonding
84 between the fibers making chitin less crystalline, but it could also eliminate residual proteins contained
85 in the raw chitin biomasses while maintaining a high molecular weight (Shamshina et al. 2016). Given
86 that controversy still exists on the IL toxicity and its degradability, deep eutectic solvents (DES) have
87 attracted the attention of the scientific community as an alternative to ionic liquids, especially in the
88 solubilization of recalcitrant biomasses such as lignocellulosic biomasses. DES are composed of at
89 least one hydrogen donor and one hydrogen acceptor at a different ratio. They share similar properties
90 with ILs such as a low melting point, a low vapor pressure, both are non-inflammable and have good
91 dissolving abilities. DES are usually claimed as less toxic than ILs because they can be composed of
92 non-toxic natural compounds (NADES) and can be produced at a cheapest price compared to ILs
93 (Zdanowicz, Wilpiszewska, and Szychaj 2018). Various applications in (bio)chemistry as catalysis
94 (Zdanowicz, Wilpiszewska, and Szychaj 2018, Singh, Lobo, and Shankarling 2012), electrochemistry
95 (Ruggeri et al. 2019) and nanomaterials production (Zhao et al. 2018) have been found for DES.
96 Recently, DES based on choline chloride have been studied in the extraction of chitin even if their
97 acidity generally leads to the production of chitin with low molecular weights (Hong et al. 2018). The

98 use of DES for the pretreatment has been hardly ever reported to date. To the best of our knowledge,
99 there is only one recent work which clearly deepens into the impact of DES pretreatment on the
100 efficiency of the chitin deacetylation reaction. The authors studied four DES with distinct
101 characteristics for chitin dissolution prior to the deacetylation reaction. They showed that DES were
102 able to disrupt chitin's strong hydrogen bonding while facilitating the NaOH penetration and,
103 consequently, the deacetylation. However, contrary to the present work, commercially available chitin
104 powder was used for the aforementioned study. Therefore, a gap still exists on the DES performance
105 over other chitin sources, and the comparison with other dissolving agents, such as ILs in order to
106 unravel the best processing route from raw chitin to high quality chitosan (Vicente et al. 2020).
107 Therefore, herein, we propose to study and compare the impact of both choline chloride/lactic acid
108 DES and [C₂mim][OAc] IL pretreatments on the efficiency of the chitin chemical deacetylation,
109 carried out on different sources (crustaceans and insects), and purity degrees (Chart 1). Both solvents
110 were chosen for their strong ability to dissolve chitin. The obtained chitosans are functionalized with
111 oleic acid under mild conditions (water/ethanol solvent, room temperature) by using *N*-ethyl-*N*'-(3-
112 dimethylaminopropyl)carbodiimide (EDC) as the coupling agent. Even if grafting fatty acids to
113 chitosan is a known procedure, it is rare to have a full characterization of the formed amide bond, as
114 esterification can be a competitive side reaction. Oleic acid has been selected for its wound healing
115 properties as it enhances the production of cytokines that help the healing process, and also for its
116 hydrophobic nature (Young-Hee et al. 2008). Indeed, it is essential to have an appropriate
117 hydrophilic/hydrophobic balance to ensure both cell-affinity and biocompatibility (Menziez and Jones
118 2010, Iacob et al. 2018).
119



120

121 Chart 1. From raw chitin biomasses to functionalized chitosans.

122

123 2. MATERIALS AND METHODS

124

125 2.1 Chitin sources

126 Three sources of chitin have been used in this study: (i) larvae from *Bombyx eri* provided by LepidUP
 127 company (Amiens, France), (ii) larvae from *Hermitia illucens* provided by SFly company (Grenoble,
 128 France) and (iii) shrimps shells from *Crangon Crangon* bought in a local market (Amiens, France).

129

130 2.2 Chemicals

131 All minerals acids and bases were used in their highest concentration possible available from VWR
 132 Europe (Briare, France) and Fischer Chemical (UK). Deionized water with a resistivity of 18.3MΩ
 133 cm, Barnsted Easy Pure RF, was used for all the experiments. 1-Ethyl-3-methylimidazolium acetate
 134 ([C₂mim][OAc], >98%) was purchased from Proionic (Grambach, Austria). Choline chloride, lactic
 135 acid and *N*-(3-Dimethylaminopropyl)-*N'*-ethylcarbodiimide hydrochloride (EDC.HCl) were supplied
 136 by Sigma-Aldrich (Streinheim, Germany). Oleic Acid (99%) was supplied by TCI Europe (Paris,
 137 France).

138

139 2.3 Instrumental analysis

140 CP-MAS ¹³C NMR spectrum was obtained at 125 MHz using a Bruker AVANCE III HD spectrometer
141 500MHz. The pulse sequence was based on cross-polarization technique. The rotation frequency of
142 sample was 15 kHz and the contact time was optimized to 2 ms with a 5 seconds delay between scans
143 to observe correctly all the carbons of chitin. The probe used allowed the use of a 2.5 mm rotor.
144 Acetylation degrees were determined by integration of the *N*-acetyl carbon atom divided by the sum of
145 the intensities of the D-glucopyranosyl carbon ring atoms. Deacetylation treatment refers to the
146 process of removal of acetyl groups from chitin and acetylation degree (DA) determines the content of
147 remaining *N*-acetyl groups. X-Ray powder diffraction (XRD) patterns were acquired using a Bruker
148 D8 Endeavor diffractometer equipped with a Cu anti-cathode (K α radiation, operating at 40 kV–40
149 mA). Patterns were collected in the 2 θ range of 10–60° with a step size of 0.03° and using a low
150 background silicon holder (Bruker AXS, C79298A3244B261). The experimental conditions used for
151 the measurement did not allow us to observe correctly the band below 10°. Crystallinity indexes (CrI)
152 were calculated from the X-ray diffractograms using the difference of intensity between the
153 amorphous area at 2 θ = 16° and the crystallinity area whose peak at its highest intensity is near 2 θ =
154 20° (Liu et al. 2012). The followed formula was: CrI = ((Intensity_{max} -
155 Intensity_{amorph})/Intensity_{max})*100). Scanning electron microscopy (SEM) was used to examine the
156 microstructure of untreated and pretreated extracted chitins, as synthesized and functionalized
157 chitosans. A small amount of dried samples (powder or flakes) was placed on double-sided carbon
158 tape adhered to aluminum SEM stubs. These were then coated with a 20 nm layer of gold and
159 examined using a Quanta 200 FEG scanning electron microscope (FEI Co., USA). The micrographs
160 were obtained with a secondary electron detector at an accelerating voltage of 2 or 5 kV. Infrared
161 spectra were obtained by using a Fourier-transform infrared (FT-IR) spectrometer (IRaffinity-1S,
162 Shimadzu) and ATR method with a germanium prism (MIRacle 10, Shimadzu). Spectra were obtained
163 in a range between 700 cm⁻¹ and 4000 cm⁻¹ at a resolution of 4 cm⁻¹ with 64 scans. Thermogravimetric
164 analysis (TGA) was recorded on a Netzsch STA 449C Jupiter thermal analyser instrument equipped
165 with a differential analysis microbalance coupled to a QMS 403 Aëolos mass spectrometer with a
166 stainless-steel capillary and a Secondary Electron Multiplier (SEV) detector (Channeltron). The
167 counting time for the mass spectrometer was 20 ms per (m/z) value (scanning width: m/ z=10–150
168 amu) with a resting time of 1 s. The samples (approximately 20 mg of each compound) were heated in
169 an alumina crucible under argon, by equilibrating at 25 °C, and followed a ramp at 5 °C/min up to 800
170 °C and an isotherm under air atmosphere for 30 min (Flow rate: 50 mL/min). Elemental (C, H, N, S)
171 characterization was performed in a Thermo Flash 1112 analyzer. Samples were placed in Ag capsules
172 and pyrolyzed at 1070 °C under a He flow. The produced gases flowed through a reducing bed of
173 carbon black that transforms all CO_x into CO. Subsequently, the gases flowed through a polar
174 chromatographic column that separates CH₄ from CO and the latter is detected and quantified using a
175 thermal conductivity detector calibrated with sulphanilamide.

176

177 **2.4 Extraction of chitin from insect and shrimp sources**

178 *Bombyx eri* larvae were frozen alive overnight. Then *Bombyx eri* larvae were boiled and extruded with
179 a household juice extractor to separate the solid biomass composed mainly of chitin, minerals and
180 proteins and a liquid composed mainly of proteins and lipids. After filtration, the solid fraction was
181 washed with Milli-Q water, ethanol and then acetone to obtain *Bombyx eri* larvae cuticles (**BE-0**).
182 Although the extraction of shrimp's carapaces and *Hermitia illucens*'s cuticles was not done by
183 ourselves, similar extraction procedures were applied on both sources. *Bombyx eri* larvae cuticles,
184 shrimp shells and *Hermitia illucens* powder were washed several times with water followed by ethanol
185 and acetone and dried under vacuum to obtain unpurified chitin called **BE-0**, **S-0** and **HI-0**
186 respectively. These unpurified chitin biomasses were first demineralized with a 1M hydrochloric acid
187 solution at 95° for 35 minutes and neutralized with Milli-Q water until neutral pH. Then, the obtained
188 demineralized chitins were deproteinized with 1M NaOH solution at 80 °C for 24 h, neutralized with
189 Milli-Q water, washed with ethanol and acetone and then dried under vacuum to obtain purified chitin
190 called **BE-2** (yield:25.2%), **S-2** (yield: 26.7%) and **HI-2** (yield: 25.5%) respectively.

191

192 **2.5 Nitrogen content using Kjeldahl method**

193 Nitrogen contents of the chitin samples before and after [C₂mim][OAc]- and DES-pretreatment were
194 determined using the Kjeldahl method adapted from the literature (Díaz-Rojas et al. 2006). In brief,
195 100 mg of chitin biomasses was dissolved in 10 mL of concentrated sulfuric acid in presence of
196 Kjeldahl catalyst (9 % CuSO₄.5H₂O). After heating at high temperature (>350 °C) until the solution
197 became transparent without white smoke, the solution was cooled at room temperature. 70 mL of
198 distilled water and 70 mL of a solution of NaOH 40 % (w/w) were added and distilled. The distillate
199 was trapped in a 30 mL of Tashiro indicator solution and finally titrated with a solution of HCl 0.1M
200 until the solution became violet. Chitin and protein contents determination are detailed in the
201 electronic supporting information.

202

203 **2.6 RTIL-pretreatment of sample**

204 **BE-0**, **BE-2**, **HI-0**, **HI-2**, **S-0** and **S-2**, have been pretreated with [C₂mim][OAc] as already described
205 by some of us (Huet et al. 2020, Husson et al. 2017). In brief, 5 g of chitin biomass was introduced in
206 250 mL of [C₂mim][OAc] (0.2 % w/v) at 110 °C for 40 minutes under stirring. Then, 250 mL of MQ
207 water was added to regenerate chitins. After filtration, the resulting solid was washed by a repetition of
208 filtration and sonication with MQ water and lyophilized. Chitin obtains were called **BE-0-IL**, **BE-2-**
209 **IL**, **HI-0-IL**, **HI-2-IL**, **S-0-IL**, and **S-2-IL** respectively. Yields are summarized in Table 1.

210

211 **2.7 DES-pretreatment of sample**

212 Choline chloride (CC) was mixed with lactic acid (LA) in a molar ratio of 1:2 inside a glass bottle.
213 The mixture was stirred overnight at 50°C to homogenize the solution before use. Then, **BE-0**, **BE-2**,

214 **HI-0, HI-2, S-0** and **S-2** were pretreated with CC/LA DES. In brief, 2 g of chitin biomass was
215 introduced in 100 mL of DES (0.2 % w/v) at 110 °C for 2 h under stirring. Then, 250 mL of Milli-Q
216 water was added and filtered. The resulting solid was washed by a repetition of filtration and
217 sonication with Milli-Q water and finally lyophilized. Chitins obtained were called **BE-0-DES, BE-2-**
218 **DES, HI-0-DES, HI-2-DES, S-0-DES** and **S-2-DES** respectively. Yields are summarized in Table 1.

219

220 *2.8 Deacetylation of sample*

221 In a typical experiment, 500 mg of chitin from **BE, HI** or **S** sources was added to 25 mL of a solution
222 of NaOH (50 % w/v) and the mixture was heated overnight (16 h) at 100°C under stirring. The solid
223 was filtered and washed with MQ water until neutral pH. The recovered solid was then sonicated in
224 MQ water and filtrated, this step was repeated 5 times. The resulting chitosan was finally washed
225 successively with ethanol and acetone and dried under vacuum pump. Yields of **dBE, dHI** and **dS** are
226 summarized in Table S1 (ESI) and Figure 3.

227

228 *2.9 Oleic acid-grafted chitosan*

229 Before chemical modification, all chitosan samples were grinded with a ball milling RETSCH MM400
230 (150W) in a 50mL stainless steel bowl (1.4112) with a stainless ball of 25mm diameter during 2min at
231 25Hz. The grafting has been processed using a slightly modified method reported by Niemczyk et al
232 (Agata Niemczyk et al. 2019). In a typical experiment 600 mg of chitosan were solubilized into 60mL
233 solution of 0.1M hydrochloric acid and ethanol 2:1 (v/v) and stirred for 3 hours at room temperature to
234 ensure a complete solubilization of the chitosan. The pH was then raised between 5 and 6. In parallel,
235 1.2g of EDC.HCl and 2mL of oleic acid were mixed with ethanol (20 mL), stirred for 3h at room
236 temperature and added dropwise to the chitosan solution. The mixture was stirred for 24h at room
237 temperature and the solvents were then eliminated under reduced pressure. The residual solid was
238 filtered and washed several times with hot ethanol. The functionalized chitosan was then stirred in hot
239 cyclohexane for a day and then sonicated, filtered and dried under vacuum to remove all traces of
240 adsorbed oleic acid.

241

242 *2.10 Degrees of substitution*

243 Degrees of substitution (DS) of chitosan samples have been evaluated thanks to the data obtained from
244 the elemental analysis and following the Inukai's equation adapted to oleic acid: $DS = ((C/N) - (C/N)_{initial})/n$. (Inukai et al. 1998) Where (C/N) is the ratio between the carbon and nitrogen content
245 of the product after grafting and (C/N)_{initial} is the ratio of carbon and nitrogen content of the chitosan
246 before grafting. "n" represents the number of carbons added to one glucosamine unit by grafting oleic
247 acid which is 18 in this case. The degrees of substitution (DS) of **OA-dBE-0-IL, OA-dBE-2, OA-**
248 **dBE-2-IL, OA-dBE-2-DES, OA-dS-2-IL** are summarized in Table 2.

250

251 **3. RESULTS AND DISCUSSION**

252

253 **3.1 Extraction process, composition and purity**

254 Chitins have been extracted using the classical chemical method involving two steps,
 255 demineralization and deproteinisation reactions, respectively (Huet et al. 2020). Two insect sources
 256 have been selected: (i) *Bombyx eri* larvae (**BE**) for which the extraction has already been reported by
 257 some of us (Huet et al. 2020) and (ii) the black fly soldier larvae *Hermetia illucens* (**HI**), one of the
 258 most promising insects studied as a new source of proteins/lipids for fish farming (Nogales-Mérida et
 259 al. 2019). Insects are also promising alternative for chitin/chitosan production as their breeding can be
 260 controlled and can produce homogenous chitin quality. Moreover, chitin biomass from insects
 261 contains less minerals than that of crustaceans (<6%) which means that at an industrial level, this
 262 difference results in a beneficial reduction in the cost, in the duration of the process and in the
 263 pollution caused by the wastewater treatment during the demineralization step. For comparison, this
 264 extraction has also been realized on shrimp shells (**S**). The samples were labelled “**0**” for the clean raw
 265 chitin biomasses (**BE-0**, **HI-0**, **S-0**) and “**2**” for the extracted chitins after the consecutives
 266 deproteinization and demineralization steps (**BE-2**, **HI-2** and **S-2**). The chitin purity, ash and protein
 267 contents for all samples are reported Table 1. Indeed, chitin contents of **BE-2**, **HI-2** and **S-2** are $93.3 \pm$
 268 0.4 , 95.0 ± 2.8 and 90.5 ± 0.4 % respectively. These results show that this extraction, adapted for
 269 crustacean biomass, is also working on both insect biomasses for whom the ash and protein contents
 270 are lower than 0.5%. In addition, as shown in our first study, the demineralization step is not always
 271 required on insect biomass and could be skipped; however, in order to better compare **S-2** with **BE-2**
 272 and **HI-2**, the demineralization step was done for all samples (Huet et al. 2020).

273

274 Table 1. Characterization data of raw biomasses, extracted chitins and pretreated samples from insect cuticles
 275 and shrimp shells sources.

Chitin source	Water^a (%)	Lipid^b (%)	Ash content^a (%)	Protein^c (%)	Chitin purity^c (%)	CrI^d (%)	Yield^e (%)
<i>Bombyx eri</i>							
BE-0	6.0 ± 0.06	0.3	1.9 ± 0.02	45.8 ± 0.5	45.0 ± 0.5	ND	-
BE-0-IL	8.3 ± 0.08	ND	0.4 ± 0.01	31.8 ± 5.6	59.5 ± 5.6	ND	60
BE-0-DES	4.2 ± 0.04	ND	1.5 ± 0.02	34.1 ± 3.5	60.2 ± 3.5	ND	45
BE-2	4.0 ± 0.04	0	0.3 ± 0.01	0 ± 0.4	93.3 ± 0.4	78 ± 3.9	-
BE-2-IL	6.9 ± 0.07	ND	1.0 ± 0.01	0 ± 6.1	99.0 ± 6.1	76 ± 3.8	93
BE-2-DES	2.5 ± 0.03	ND	0.3 ± 0.01	0.3 ± 2.2	96.8 ± 2.2	92 ± 4.6	65
<i>Hermetia illucens</i>							
HI-0	4.8 ± 0.05	1.14	1.8 ± 0.02	60.3 ± 0.1	33.0 ± 0.1	ND	-

HI-0-IL	3.9 ± 0.04	1.14	1 ± 0.01	45.6 ± 2.4	48.4 ± 2.4	ND	50
HI-0-DES	5.0 ± 0.05	ND	0.0	52.2 ± 0.7	42.8 ± 0.7	ND	55
HI-2	4.5 ± 0.05	0.46	0.5 ± 0.01	0.1 ± 2.8	95.0 ± 2.8	84 ± 4.2	-
HI-2-IL	5.5 ± 0.06	ND	0.2 ± 0.01	0	94.2 ± 1.1	76 ± 3.8	95
HI-2-DES	4.1 ± 0.04	ND	0.7 ± 0.01	0	100.0 ± 0.9	90 ± 4.5	68
<i>Shrimp shells</i>							
S-0	9.2 ± 0.09	0	30.4 ± 0.30	47.8 ± 1.5	22.9 ± 1.5	ND	-
S-0-IL	11.0 ± 0.11	0	34.0 ± 0.34	20.6 ± 2.33	36.2 ± 2.33	ND	79
S-0-DES	8.13 ± 0.08	ND	12.6 ± 0.13	24.8 ± 2.6	54.5 ± 2.6	ND	56
S-2	7.0 ± 0.07	ND	0.5 ± 0.01	2.0 ± 0.4	90.5 ± 0.4	82 ± 4.1	-
S-2-IL	8.7 ± 0.09	0	0.4 ± 0.01	2.3 ± 5.1	91.2 ± 5.1	77 ± 3.9	92
S-2-DES	7.1 ± 0.07	0	0.03 ± 0.01	0	96.6 ± 1.8	92 ± 4.6	65

276 (a) determined using thermogravimetric analysis under nitrogen atmosphere from 50 to 800 °C followed by an isotherm at
277 800 °C under air for 30 minutes; (b) determined using the Soxhlet extraction method; (c) evaluated using the Kjeldahl
278 method and using the methodology described by Diaz-Rojas et al. (Díaz-Rojas et al. 2006); (d) calculated using X-Ray
279 diffractograms and the amorphous subtraction region method; (e) the yield of chitin was determined according to the weight
280 difference of the raw material and extracted/pretreated chitin. ND: Not determined.

281

282 **3.2 Impact of the pretreatment: IL versus DES**

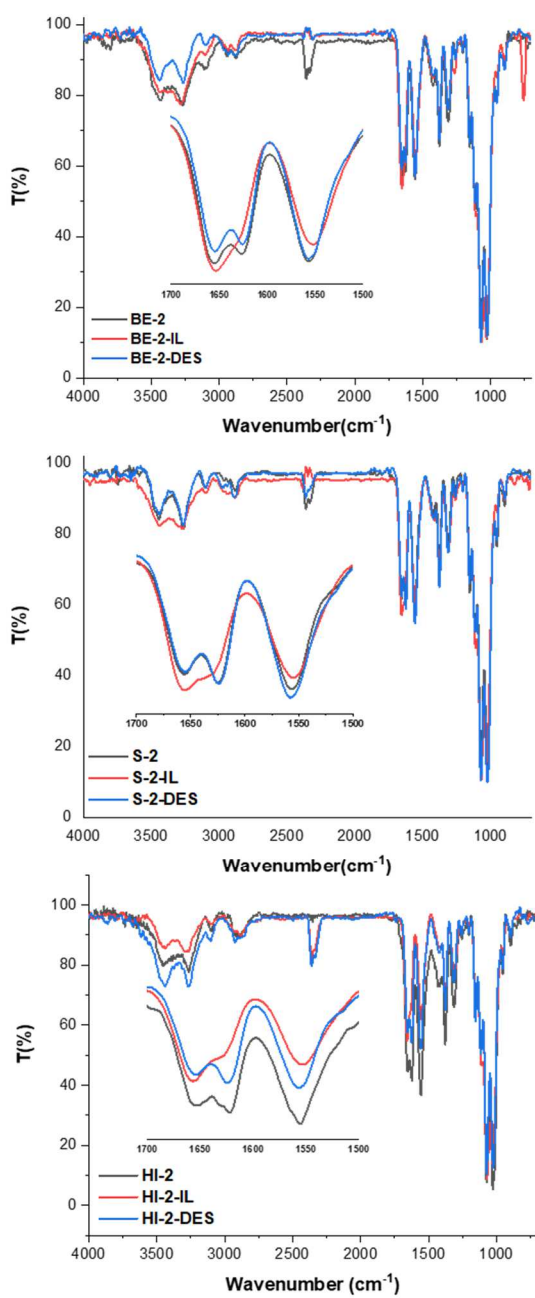
283 Among the imidazolium-based ILs, [C₂mim][OAc] is probably one of the most efficient to
284 solubilize chitin under mild conditions (110 °C for 40 min). It has already been demonstrated that
285 [C₂mim][OAc] can modify the supramolecular structure by disrupting the hydrogen network in the
286 chitin structure leading to a slight decrease in the crystallinity indexes (Table 1 and see also ESI,
287 Figures S1-S3). Since the raw biomasses **BE-0**, **HI-0** and **S-0** contain a large amount of proteins and
288 minerals, the crystallinity indexes CrI, before and after pretreatment were not evaluated. This
289 supramolecular modification by IL depends on the β parameter of the Kamlet Taft parameters either
290 called neat basicity which must be superior to 0.5 (Shamshina 2019). The higher the β Kamlet-Taft
291 parameter is, the higher the IL will be able to solubilize recalcitrant polymers such as chitin. Purified
292 chitins **BE-2**, **S-2** and **HI-2** were partially soluble in [C₂mim][OAc] whereas the raw biomasses (**BE-**
293 **0**, **S-0** and **HI-0**) were not soluble. This result can be firstly explained by the presence of a large
294 amount of proteins in the raw biomasses making it difficult for the IL to access the fibers. Secondly,
295 the physico-chemical properties of the biopolymer such as the molecular weight (MW), or the DA are
296 also of great importance and will affect its solubility (Julia L. Shamshina 2019). Indeed, as
297 depolymerization occurred during the 2-step extraction process, the MW of the purified chitin should

328 be lower than the one contained in the raw biomasses. α -Chitin organizes itself with an anti-parallel
329 pattern between fibers, which can be seen on FTIR spectra by the 2 characteristic peaks at 1660 cm^{-1}
330 and 1620 cm^{-1} of the C-O bonding of the amide function (Figure 1). As described in our previous
331 studies, $[\text{C}_2\text{mim}][\text{OAc}]$ pretreatment partially solubilizes chitin, breaking hydrogen bonds and
332 disrupting its supramolecular structure. The chitin α -pattern is not observable anymore on the FTIR
333 spectrum (Figure 1). Similar trends were observed on **BE-2-IL**, **S-2-IL** and **HI-2-IL** suggesting that
334 the pretreatment was effective on all those sources. Due to the large amount of residual proteins in the
335 raw materials, it was difficult to draw any conclusion from the FTIR spectra concerning the impact of
336 the pretreatment and structural changes on **BE-0-IL**, **S-0-IL** and **HI-0-IL**. Indeed, peptide bonding of
337 proteins also appears at 1660 cm^{-1} (See supporting information figure S4). However, we have
338 previously demonstrated that an IL pretreatment on raw biomasses (**BE** and **S** sources), prior to
339 enzymatic hydrolyses, leads to higher yields in *N*-acetylglucosamine and *N, N'*-diacetylchitobiose,
340 suggesting a better access to the fibers than untreated materials, thus such pretreatment entailing an
341 impact on the supramolecular structures of the chitin fibers (Huet et al. 2020). The ratio
342 chitin/proteins/minerals for all samples were then evaluated using thermogravimetric analysis and the
343 Kjeldahl method (Díaz-Rojas et al. 2006). The obtained data from the raw materials and listed Table 1,
344 indicate the partial removal of some proteins, especially in the case of shrimp shells source where 56%
345 of the proteins were eliminated. On the contrary, no effect on the minerals content is observed,
346 regardless of the source.

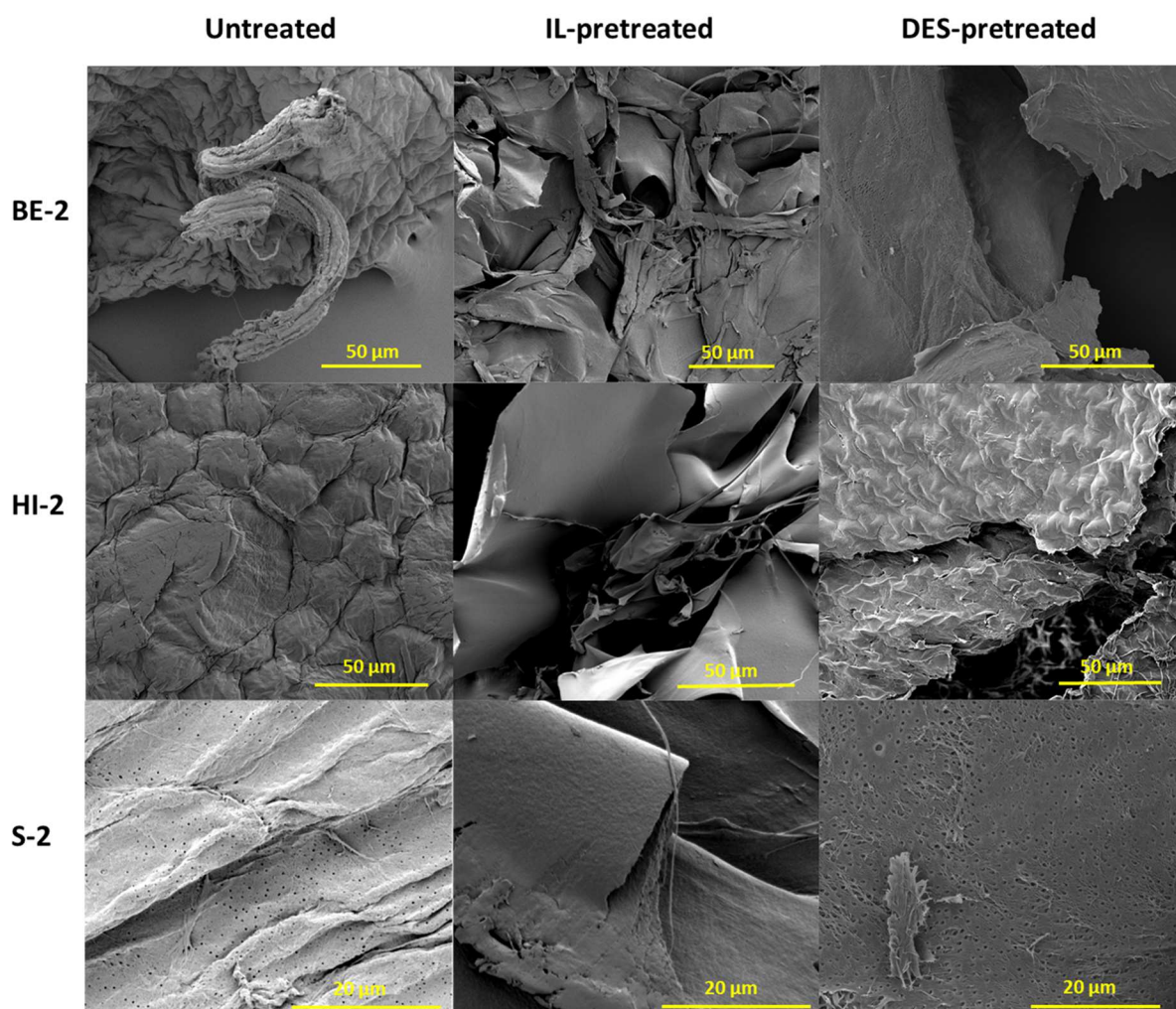
347 DES based on choline chloride as a hydrogen bond acceptor, and organic acids (i.e. malonic acid,
348 malic acid or lactic acid) as hydrogen bond donors are interesting solvents for polysaccharides
349 dissolution and extraction processes of biomasses (Chen and Mu 2019). Chitin can be successfully
350 extracted using organic acid based DES under mild conditions and short reaction times compared to
351 the traditional chemical method (Zhu et al. 2017). However, depolymerization collaterally occurs, and
352 these fast extractions using organic acid based DES generally lead to low molecular weight chitins
353 depending on the nature of the organic acid, the temperature and the duration of the reaction (Bradić,
354 Novak, and Likozar 2020). In this study, choline chloride-lactic acid (CC:LA) in a 1:1 ratio was
355 chosen to pretreat both marine and insect raw materials, as well as pure chitins. 2h of pretreatment was
356 used for the maximum preservation possible of the molecular weight of the polymer, and contrary to
357 the majority of related literature, our samples were not ground. The FTIR spectrum before and after
358 pretreatment of raw materials and extracted chitins were performed and are reported in Figure 1
359 (extracted chitins) and in the ESI Figure S4 (raw materials). Contrary to the IL-pretreatment, the α -
360 pattern in chitin has been preserved during the pretreatment, since the two characteristic peaks at 1660
361 cm^{-1} and 1620 cm^{-1} of the amide C-O bonding are still observed on the FTIR spectrum of the DES-
362 pretreated extracted chitin. However, similarly to IL-pretreated raw materials, DES-pretreated raw
363 materials still contain a huge amount of proteins, hindering these two characteristic peaks. Contrary to
364 IL-pretreatments, DES-pretreatments on pure chitins induce a significant increase of the CrI due to the

335 acidic nature of the DES, partially removing the amorphous regions. CrI are listed in Table 1. It is
336 worth noting that the **BE-2-DES**, **HI-2-DES** and **S-2-DES** CrI are higher than 90 %. These values are
337 similar to the one owned by chitin nanocrystals (Gueye et al. 2016). These results are fully in line with
338 those obtained by FTIR where α -structures are maintained for these samples after the DES
339 pretreatment. The amorphous regions removal can be also confirmed with the yields of pretreatment
340 summarized in Table 1. By comparison to the obtained yields after IL pretreatment of the extracted
341 chitins (**BE-2-IL**, **HI-2-IL** and **S-2-IL**) and the one obtained after DES pretreatment (**BE-2-DES**, **HI-**
342 **2-DES** and **S-2-DES**), important differences can be observed. For example, a yield of 93 % has been
343 calculated for **BE-2-IL** whereas only a 65 % has been determined for **BE-2-DES**. Since **BE-2** does not
344 contain minerals and proteins, the observed loss in mass necessarily comes from the elimination of the
345 amorphous regions. This is also the case for **HI-2** and **S-2** samples (95 % versus 68 % and 92 %
346 versus 65 % respectively). The ratio chitin/proteins/minerals for all DES-pretreated samples were also
347 evaluated and data are listed in Table 1. The obtained data indicate a lower effectiveness of the DES
348 pretreatment to remove proteins. Indeed, a 48 % of the proteins were eliminated in the case of shrimp
349 shells source versus a 56% after the IL-pretreatment. However, due to the acidic nature of the DES,
350 almost 60% of the mineral content of the shrimp shell samples were eliminated.

351 Although both pretreatments are able to partially extract chitins form biomasses these data also
352 suggest that DES and IL do not act in the same way. Indeed, from our previous study, it has been
353 reported that [C₂mim][OAc] pretreatment creates delaminated structures, detached thin sheets and,
354 occasionally, separated microfibrils, from a denser and smoother untreated chitin material, as observed
355 by SEM images (Figure 2 and see also ESI Figure S5) (Huet et al. 2020, Husson et al. 2017). On the
356 contrary, SEM images corresponding to DES-pretreated extracted chitins (Figure 2) or DES-pretreated
357 raw materials (Figures S5) do not show real changes in morphology compared to untreated chitins.



358
 359 Fig. 1 ATR-FTIR spectra of extracted chitins (black lines), IL-pretreated extracted chitins (red lines) and DES-
 360 pretreated extracted chitins (blue lines) from BE, HI and S sources. Insets: Zoom of the 1700-1500 cm⁻¹ range.
 361
 362



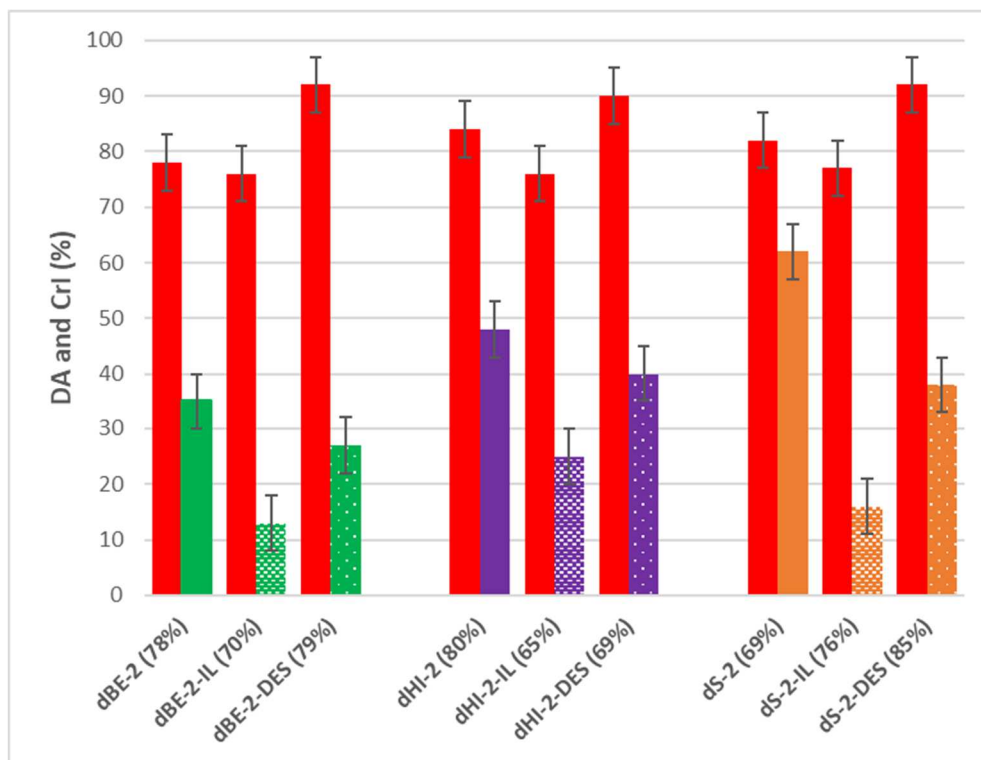
363
 364 Fig. 2 SEM images of extracted chitins, IL-pretreated extracted chitins and DES-pretreated extracted chitins
 365 from BE, HI and S sources.
 366

367 3.3 Synthesis of chitosans

368 The reaction effectiveness is strongly dependent on the polymer crystallinity and complete
 369 deacetylation is difficult to achieve without a specific procedure. Indeed, it has been shown that a
 370 highly crystalline chitin leads preferentially to a low deacetylation degree (Dhillon et al. 2013). By
 371 opening the crystalline structure of chitin, it is possible to make it more permeable to alkaline
 372 solutions, increasing the accessibility of the acetylated units to the alkali and facilitating their
 373 deacetylation. It is also important to underline that the chitosan quality also depends on the raw
 374 materials. In this study, chitosan preparations were carried out using heterogeneous conditions and the
 375 classical alkali deacetylation in concentrated NaOH (50 %, w/v) at 100 °C for 16 h, in one cycle of
 376 reaction. The determination of the degree of acetylation (DA) has been used to compare the ability of
 377 both pretreatments to enhance the efficiency of the reaction. This parameter is one of the most
 378 important since it affects the chitosan properties. DAs have been determined using solid-state CP-
 379 MAS ¹³C NMR and data are reported in the ESI Figures S6-S11 (see also ESI, table S1). The impact

380 of the pretreatment has been correlated with the obtained DA values after deacetylation of **S-2** and
381 IL/DES pretreated **S-2**. Indeed, chitosan from **S-2** presents a DA of $62 \pm 3.1 \%$ while chitosans
382 obtained from **S-2-IL** and **S-2-DES** were of $16 \pm 0.8 \%$ and $38 \pm 1.9 \%$ respectively. This tendency
383 was significantly less marked with the two others sources: the DA value after deacetylation of **BE-2**
384 was of $35 \pm 1.8 \%$ while after IL and DES pretreatment the values were of $13 \pm 0.7 \%$ and $27 \pm 1.4 \%$
385 respectively; and the DA value after deacetylation of **HI-2** was of $48 \pm 2.4 \%$ while after IL and DES
386 pretreatment the values were of $24 \pm 1.2 \%$ and $40 \pm 2.0 \%$ respectively. These results suggest that (i)
387 the deacetylation efficiency is strongly dependent on the raw biomasses sources and seem to be more
388 favorable without pretreatment, in the case of extracted chitins from insect sources; and (ii) the IL-
389 pretreatment considerably enhances the deacetylation efficiency whatever the sources (Figure 3). This
390 last observation is consistent with the slight decrease of the CrI. However, contrary to what is stated in
391 the literature, our DES-pretreated samples have the highest CrI (>90%) together with lower DA values
392 than the untreated samples. These results can be attributed to the fact that the DES-pretreatment
393 removed part of the amorphous regions leading to low MW chitins, more sensitive to the deacetylation
394 process.

395 On the other hand, deacetylation reactions performed on raw biomasses **S-0** and IL/DES-pretreated **S-**
396 **0** provided DA values of $14 \pm 0.7 \%$, $19 \pm 1.0 \%$ and $20 \pm 1.0 \%$ respectively. Pretreatments do not
397 seem to have any impact on the deacetylation efficiency when working with unpurified chitins.
398 However, even though DA values are very low, high ash contents determined by TGA are still present
399 on chitosan samples (up to 28%, see ESI Table S1). Same results can be observed in the case of the
400 raw **BE** biomass. Indeed, after deacetylation of the untreated **BE-0**, a DA value of $23 \pm 1.2 \%$ was
401 obtained, while after IL and DES pretreatment DA values of $17 \pm 0.9 \%$ and $18 \pm 0.9 \%$ were
402 achieved. But, contrary to chitosan obtained from the **S-0** source, TGA data of untreated and
403 pretreated **BE-0** samples (Table 1) together with solid state ^{13}C NMR spectra (See ESI Figure S6)
404 indicated that there were no impurities in the chitosan obtained from IL and DES-pretreated **BE-0**.
405 Finally, solid-state CP-MAS ^{13}C NMR spectra of deacetylated raw biomasses **HI-0** and IL-pretreated
406 **HI-0** displayed higher DA values ($43 \pm 2.2 \%$ and $44 \pm 2.2 \%$ respectively) than deacetylated DES-
407 pretreated **HI-0** ($24 \pm 1.2 \%$). However, solid-state CP-MAS ^{13}C NMR spectra also reveal the presence
408 of a large amount of impurities with a broad peak in the 30-40 ppm range as already observed by Song
409 and co-worker during the deacetylation of extracted chitin from blowfly (Song et al. 2013). These
410 impurities were also present in the solid-state CP-MAS ^{13}C NMR spectra of deacetylated **HI-2** and
411 IL/DES-pretreated **HI-2**.



412
 413 Fig. 3 Impact of IL/DES pretreatment on chitosan synthesis: DA values for extracted **BE-2** (green bars), **HI-2**
 414 (purple bars) and **S-2** (yellow bars) sources; CrI values (red bars) for **BE-2**, **HI-2** and **S-2** sources. Values in
 415 parenthesis indicate the yield of deacetylation reactions.

416
 417 The obtained yields based on the recovered mass after deacetylation of the extracted chitins
 418 and IL/DES-pretreated extracted chitins (**BE-2**, **HI-2** and **S-2**) are between 65 and 85 % and are listed
 419 Table S1 (ESI). These values are consistent with the calculated DAs, purity degrees of each starting
 420 material and the mass loss corresponding to the *N*-acetyl groups. In the cases of untreated and IL/DES-
 421 pretreated **BE-0** raw biomasses, as expected lower yields have been obtained (25, 35 and 51 %
 422 respectively). These results are mostly due to the lower chitin contents (between 45 and 60 %) and the
 423 removal of the proteins. Yields obtained from untreated and IL/DES-pretreated **HI-0** and **S-0** raw
 424 biomasses are slightly higher than **BE-0** sources due to the presence of impurities and minerals
 425 detected by solid state ¹³C NMR and TGA respectively.

426 Since the solubility in acidic media together with the viscosity are strongly dependent on the
 427 MW and the DA, chitosans obtained from untreated and IL/DES-pretreated chitins were solubilized in
 428 1 % acetic acid at a concentration of 10 mg/mL. Pictures of the solution have been reported Figure
 429 S12 (ESI). It is important to stress that the solubility study was performed on non-milled samples. As
 430 expected, and due to the large amount of impurities together with relatively high DA (up to 48 %),
 431 chitosans from **HI** (raw material and extracted chitins) were not soluble in acidic media. In addition,
 432 DES pretreatment does not enhance the solubility of the obtained chitosan compare to untreated
 433 samples despite their lower DA values. This is probably due to the high CrI of the chitin after
 434 pretreatment. Among all the synthesized chitosans, **dBE-2-IL** offers the highest transparency followed

435 by **dS-2-IL**. These results can be ascribed to a very high sample purities and to low DA values ($13 \pm$
436 0.7% and $16 \pm 0.8 \%$ respectively). In addition, compared to **dBE-0-IL** and **dS-0-IL** samples, **dBE-2-**
437 **IL** and **dS-2-IL** were synthesized from extracted chitins that underwent partial depolymerization
438 during the extraction procedure leading to lower MW chitosans.

439

440 **3.4 Selective amidation of chitosan with fatty acid**

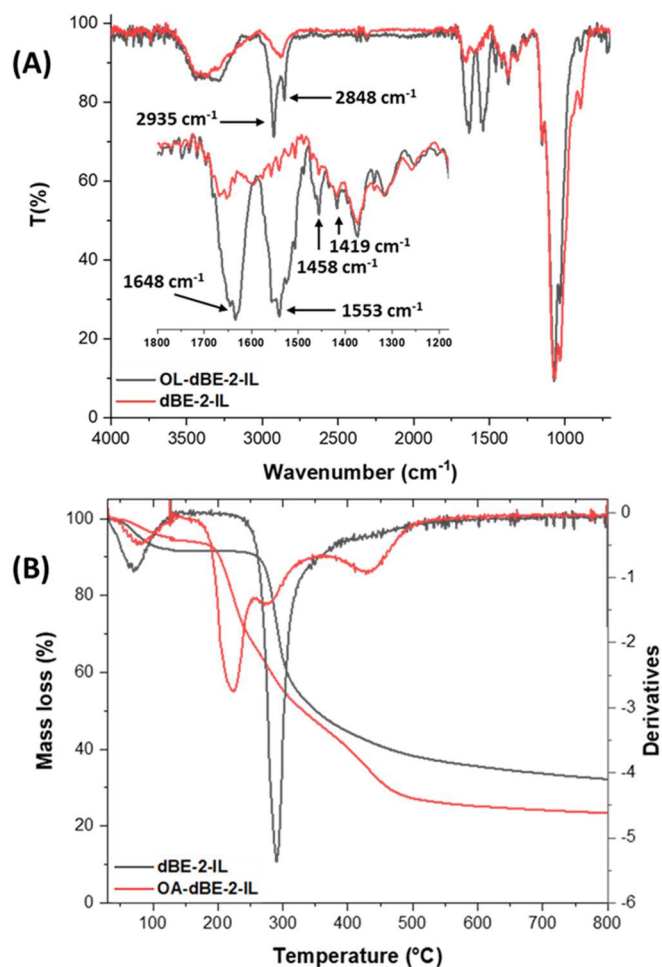
441 Considering the previous results and taking into account their purity and solubility properties,
442 amidation reactions were performed on chitosans **dBE-2**, **dBE-2-IL**, **dBE-2-DES**, **dBE-0-IL** and **dS-**
443 **2-IL**. A fatty acid has been selected for the chitosan modification since it is well known that chitosan-
444 fatty acid derivatives are considered as amphiphilic products, suitable for biomedical applications
445 (Agata Niemczyk et al. 2019, Bonferoni et al. 2014, Du et al. 2009). Indeed, these derivatives possess
446 unique physico-chemical properties, including high thermal stability, antimicrobial activity or
447 improved lubricity (Agata Niemczyk, El Fray, and E. Franklin 2015, A Niemczyk et al. 2016). The
448 grafting has been processed using a modified method reported by Niemczyk et al (Agata Niemczyk et
449 al. 2019) in the presence of EDC activation enabling the carboxylic groups to react with a nucleophile
450 by controlling the pH. Given that $-\text{NH}_2$ groups are stronger nucleophiles than $-\text{OH}$ groups, the *N*-
451 acylation is favored and the *O*-acylation become almost impossible. The authors have demonstrated
452 that by controlling the pH of the reaction (4.5-5), it was possible to partially protect the amino groups
453 leading to *O*- and *N*-acylated chitosan. They have also reported a correlation between the fatty acid
454 saturation (chain mobility) and the degree of substitution. Therefore, oleic acid, a mono-unsaturated
455 omega-9 fatty acid, was chosen for this study and the pH of the reaction was raised to 6 in order to
456 promote the *N*-acylation. To improve the reaction and facilitate its solubility in the reaction medium,
457 chitosan samples were milled into powder. In addition, to provide reliable degrees of substitution,
458 adsorbed oleic acid on the chitosan surface was eliminated by washing abundantly the final product
459 with hot ethanol, followed by cyclohexane washing aided by ultrasounds.

460

461 FTIR spectra of chitosans and chitosan-fatty acid derivatives obtained from **BE** and **S** sources
462 are presented in Figure 4 and Figures S13 to S16 in the ESI. As shown in Figure 4, concerning **dBE-2-**
463 **IL** and **OA-dBE-2-IL** IR spectra, the formation of the amide bond has been highlighted by the
464 increased intensity of the band at 1648 cm^{-1} ($\text{C}=\text{O}$ stretching vibration) and the presence of the band
465 1553 cm^{-1} (NH bending vibration, amide II band). A significant increase in absorption centered at 2935
466 and 2849 cm^{-1} together with the presence of the low bands at 1458 and 1419 cm^{-1} corresponding to the
467 alkyl chain are also observed. In addition, no band around 1740 cm^{-1} as described by Le Tien et al. (Le
468 Tien et al. 2003) was observed suggesting that the *O*-acylation did not occur during the reaction. Same
469 results have been observed for the functionalized chitosans **OA-dBE-0-IL** and **OA-dS-2-IL** (ESI,
470 figures S13 and S16), while in the case of the grafting performed with **dBE-2** and **dBE-2-DES** (ESI,
471 Figures S14 and S15), the reaction seems to be less efficient.

472

473



474

475 Fig. 4 (A) FTIR spectra of **dBE-2-IL** (black line) and **OA-dBE-2-IL** (red line). Inset: zoom of the 1200-1800
 476 cm^{-1} region. (B) Thermogravimetric and differential thermal analysis **dBE-2-IL** (black line) and **OA-dBE-2-IL**
 477 (red line) under argon atmosphere from 50 to 800 °C.

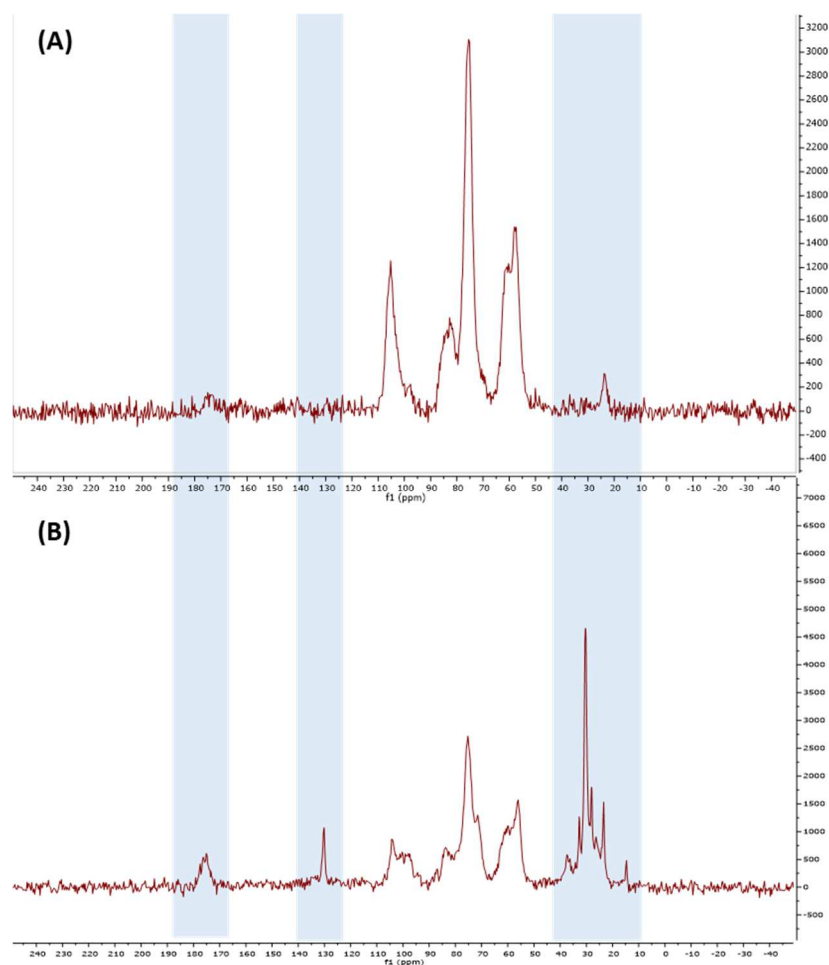
478

479 Thermal degradation of **dBE-IL-2** and **OA-dBE-IL-2** was studied using thermogravimetric
 480 analysis performed between room temperature and 800 °C (Figure 4B). As described in the literature,
 481 the thermal decomposition of chitosan occurs in 2 stages. The first one, at lower temperature (<130
 482 °C), is assigned to releasing of adsorbed water and the second one ranging from 200 to 530 °C is
 483 related to the chitosan degradation, mainly deacetylation and depolymerization reactions occurring
 484 through the cleavage of glycosidic bonds (dehydration and deamination) (Moussout, Aazza, and
 485 Ahlafi 2020, Marroquin, Rhee, and Park 2013). It was clearly observed that chitosan fatty acid
 486 derivative (**OA-dBE-IL-2**) exhibited 4 stages of degradation, the first one, below 130 °C
 487 corresponding to the loss of adsorbed water, the second from 155 °C to 250 °C is related to the OA
 488 moiety degradation, the following stage is related to the polysaccharide degradation, and nearly
 489 coincident with that of the starting chitosan, while the last stage (centered at about 450°C) is the

490 degradation of pyranose rings into short-chain organic acids (Marroquin, Rhee, and Park 2013). This
491 is something previously observed in alkyl-functionalized chitosans, in which the dangling groups may
492 form free radicals capable of reacting with the remaining chitosan backbone (Ziegler-Borowska et al.
493 2016). The obtained data confirm that the introduction of the alkyl chains in our chitosan derivative
494 reduces its thermal stability and induces a different degradation pathway.

495
496 Solid-state CP-MAS ^{13}C NMR spectra of **dB**E-IL-2 and **OA-d**BE-IL-2 are represented Figure
497 5A and 5B respectively. Concerning the chitosan, in the 50-110 ppm region, a typical resonance
498 corresponding to the anomeric carbons, the one attached to amino group and the one of the rings, are
499 observed. In addition, the carbonyl and methyl groups of *N*-acetylglucosamine units are found at 175.0
500 ppm and 23.7 ppm respectively (Duarte et al. 2001, A Niemczyk et al. 2016). After functionalization,
501 additional peaks can be observed (blue-shaded regions, Figure 5B) at 131.0 ppm and in the 10-40 ppm
502 range, and can be assigned to the C=C and to the CH_3/CH_2 of the oleic acid monounsaturated chain.
503 The shift and the increase in the intensity of the peak at 178.6 ppm can be attributed to the amide
504 formation between chitosan and the carboxylic group of oleic acid. Similar results were observed for
505 **OA-d**BE-0-IL and **OA-d**S-2-IL (Figures S17 and S17, ESI) while no additional peaks were observed
506 in the other cases.

507



508

509 Fig. 5 Solid-state CP-MAS ^{13}C NMR spectra of **dBE-IL-2** (A) and **OA-dBE-IL-2** (B).

510

511 Degrees of substitution (DS) of chitosan samples were evaluated thanks to the data obtained
512 from the elemental analysis and following the Inukai's equation adapted to oleic acid (Inukai et al.
513 1998, Lago et al. 2011). Elemental composition (weight %C, %H and %N) and DS are summarized
514 Table 2. The results clearly demonstrated that the reaction performed on IL-pretreated chitosans (**dBE-**
515 **0-IL**, **dBE-2-IL** and **dS-2-IL**) leads to higher DSs ($24.83 \pm 0.02 \%$, $27.09 \pm 0.35 \%$ and 16.83 ± 3.91
516 $\%$ respectively) compared to those obtained after reaction on untreated chitosan **BE-2** or **dBE-2-DES**
517 ($0.91 \pm 0.06 \%$ and $0.36 \pm 0.01 \%$ respectively). These data are in correlation with the FTIR spectra
518 and solid-state CP-MAS ^{13}C NMR spectra of the OA-chitosan derivatives. Another interesting point
519 concerns the DS value of **OA-dBE-0-IL** very close to one of **OA-dBE-2-IL** suggesting that this
520 biomass without any further demineralization and deproteinization step offers a sufficient chitin
521 quality to obtain chitosan almost devoid of impurities that could interfere in the coupling between
522 oleic acid and chitosan.

523

524

525

526

527

528 Table 2. Microanalysis data (%C, %H and %N) and DS.

compounds	%C	%H	%N	DS (%)
<i>Bombyx eri</i>				
dBE-0-IL	43.22 ± 0.13	6.74 ± 0.45	7.55 ± 0.07	-
OA-dBE-0-IL	52.70 ± 0.18	8.06 ± 0.02	5.17 ± 0.02	24.83 ± 0.02
dBE-2	43.23 ± 0.04	6.65 ± 0.36	7.66 ± 0.12	-
OA-dBE-2	45.10 ± 0.05	7.29 ± 0.04	6.18 ± 0.10	0.91 ± 0.06
dBE-2-IL	42.99 ± 0.01	6.86 ± 0.33	7.69 ± 0.02	-
OA-dBE-2-IL	51.60 ± 0.10	7.98 ± 0.18	4.93 ± 0.04	27.09 ± 0.35
dBE-2-DES	42.99 ± 0.21	6.86 ± 0.39	7.78 ± 0.07	-
OA-dBE-2-DES	43.90 ± 0.19	7.06 ± 0.14	6.81 ± 0.04	0.36 ± 0.01
<i>Shrimp shells</i>				
dS-2-IL	42.90 ± 0.16	6.46 ± 0.03	7.44 ± 0.06	-
OA-dS-2-IL	54.00 ± 3.35	8.31 ± 0.47	5.49 ± 0.64	16.83 ± 3.91

529

530 4. CONCLUSIONS

531 IL and DES solvent became very popular in the field of polysaccharides for their strong ability to
532 extract and to dissolve these biopolymers, particularly for chitin. Therefore, it can be hard to
533 distinguish the real advantages of using IL or DES in the treatment of chitin biomasses. The
534 comparative study conducted between choline chloride/lactic acid DES and $[\text{C}_2\text{mim}][\text{OAc}]$ IL in this
535 manuscript highlights that even if both solvents are able to remove proteins from raw biomasses, IL
536 seems to be more efficient (up to 56% for shrimp biomass). The acidic nature of CC/LA DES solvent

537 can also remove a large mineral content (42%, **S-0-DES**) for shrimp shells whereas IL remains
538 inefficient. In addition, IL and DES do not have the same impact on the chitin's supramolecular
539 structure. Indeed, the α -pattern is not anymore observable on the FTIR spectrum of extracted chitin
540 whatever the sources, suggesting the high ability of IL to modify the chitin's structure whereas the α -
541 polymorphism remains present with the DES-pretreatment. The high CrI (> 90%) for the purified
542 chitin **BE-2-DES**, **HI-2-DES** and **S-2-DES** indicates the removal of amorphous region and
543 consequently a strong depolymerization process leading to low molecular weight. On the contrary, IL
544 has less effect on the chitin depolymerization and is a suitable solvent to keep chitin with a high
545 molecular weight (Wineinger et al. 2020) than DES. The slight decrease in the CrI value for **BE-2-IL**,
546 **HI-2-IL** and **S-2-IL** compared to untreated biomass has a direct impact on the deacetylation step
547 suggesting that chitin amorphization is one key to afford chitosan with low acetylation degree. With
548 the highest CrI value, DES-samples also led to chitosan with higher deacetylation degree than
549 untreated samples but inferior to IL-pretreatment. Keeping in mind that amorphization is one key-step
550 to obtain chitosan with low DA, it should be expected a higher DA for all DES-samples. The low
551 molecular weight combined to the fact that the acidic DES was able to protonate the few NH₂ groups
552 present in chitin and hence repelling the fibers by offering a better accessibility to NaOH is a
553 reasonable explanation (Mukesh et al. 2014). Among all the synthesized chitosans, **dB-E-2-IL** presents
554 the better solubility and transparency due to a very high sample purity and low DA. Finally, a selective
555 amidation reaction with oleic acid has been conducted in water media by controlling the pH. The
556 calculated DS demonstrated that chitosan obtained from chitin IL-pretreatment affords the highest
557 values from $16.83 \pm 3.91 \%$ to $27.09 \pm 0.35 \%$ whereas the grafted oleic acid on chitosan obtained
558 from DES-treatment led to poor DS value (0.36 ± 0.01 - $0.91 \pm 0.06 \%$).

559 To sum up, we demonstrated that [C₂mim][OAc] IL and CC/LA DES impact differently on chitin in
560 terms of crystallinity, molecular weight and deacetylation step. Despite its toxicity controversy, IL is a
561 suitable solvent for chitin amorphization whereas DES will preserve the α -chitin polymorphism and
562 high crystallinity. These two families of solvents offer different physical and chemical properties to
563 chitin and can cover a vast range for chitin's applications.

564

565 **ACKNOWLEDGEMENTS**

566 ANVN thanks the ministère de l'éducation nationale, de l'enseignement supérieur et de la recherche
567 for financial support. J.M.G.-D. greatly acknowledges the Spanish MINEICO for his 'Juan de la
568 Cierva Incorporation' contract, and associated research funds (ref. IJCI-2016-27789), as well as
569 financial support from the regional government of Aragón (Grupo Reconocido DGA T03_17R,
570 FEDER/UE and DGA-T03_20R).

571

572 **References**

573
574 Altiok, Duygu, Evren Altiok, and Funda Tihminlioglu. 2010. "Physical, Antibacterial and Antioxidant
575 Properties of Chitosan Films Incorporated with Thyme Oil for Potential Wound Healing
576 Applications." *Journal of Materials Science: Materials in Medicine* 21: 2227–36.
577 Anwar, Muslih, Ayu Septi Anggraeni, and M. Harisuddin Al Amin. 2017. "Comparison of Green
578 Method for Chitin Deacetylation." *AIP Conference Proceedings* 1823: 020071.
579 Aspras, Izabela, Malgorzata M. Jaworska, and Andrzej Górak. 2017. "Kinetics of Chitin Deacetylase
580 Activation by the Ionic Liquid [Bmim][Br]." *Journal of Biotechnology* 251: 94–98.
581 <http://dx.doi.org/10.1016/j.jbiotec.2017.04.015>.
582 Bajaj, Mini, Josef Winter, and Claudia Gallert. 2011. "Effect of Deproteination and Deacetylation
583 Conditions on Viscosity of Chitin and Chitosan Extracted from Crangon Crangon Shrimp
584 Waste." *Biochemical Engineering Journal* 56: 51–62.
585 Bonferoni, M. C. et al. 2014. "Ionic Polymeric Micelles Based on Chitosan and Fatty Acids and
586 Intended for Wound Healing. Comparison of Linoleic and Oleic Acid." *European Journal of*
587 *Pharmaceutics and Biopharmaceutics* 87: 101–6. <http://dx.doi.org/10.1016/j.ejpb.2013.12.018>.
588 Bradić, B, U Novak, and B Likozar. 2020. "Crustacean Shell Bio-Refining to Chitin by Natural Deep
589 Eutectic Solvents." *Green Process Synthesis* 9: 13–25.
590 Chen, Yu, and Tiancheng Mu. 2019. "Application of Deep Eutectic Solvents in Biomass Pretreatment
591 and Conversion." *Green Energy and Environment* 4: 95–115.
592 <https://doi.org/10.1016/j.gee.2019.01.012>.
593 Dhillon, Gurpreet Singh, Surinder Kaur, Satinder Kaur Brar, and Mausam Verma. 2013. "Green
594 Synthesis Approach: Extraction of Chitosan from Fungus Mycelia." *Critical Reviews in*
595 *Biotechnology* 33: 379–403.
596 Díaz-Rojas, Erika I. et al. 2006. "Determination of Chitin and Protein Contents during the Isolation of
597 Chitin from Shrimp Waste." *Macromolecular Bioscience* 6(5): 340–47.
598 Du, Yong Zhong et al. 2009. "Preparation and Characteristics of Linoleic Acid-Grafted Chitosan
599 Oligosaccharide Micelles as a Carrier for Doxorubicin." *Colloids and Surfaces B: Biointerfaces*
600 69: 257–63.
601 Duarte, M. L., M. C. Ferreira, M. R. Marvão, and João Rocha. 2001. "Determination of the Degree of
602 Acetylation of Chitin Materials by ¹³C CP/MAS NMR Spectroscopy." *International Journal of*
603 *Biological Macromolecules* 28(5): 359–63.
604 Elgadir, M. Abd et al. 2015. "Impact of Chitosan Composites and Chitosan Nanoparticle Composites
605 on Various Drug Delivery Systems: A Review." *Journal of Food and Drug Analysis* 23: 619–29.
606 Gadgey, Kishore Kumar, and Amit Bahekar. 2017. "Studies on Extraction Methods of Chitin from
607 Crab Shell and Investigation of Its Mechanical Properties." *International Journal of Mechanical*
608 *Engineering and Technology* 8: 220–31.
609 Gueye, Serigne et al. 2016. "Chronic Tubulointerstitial Nephropathy Induced by Glucosamine: A Case

610 Report and Literature Review.” *Clinical Nephrology* 86: 106–10.

611 Hamed, Imen, Fatih Özogul, and Joe M. Regenstein. 2016. “Industrial Applications of Crustacean By-
612 Products (Chitin, Chitosan, and Chitooligosaccharides): A Review.” *Trends in Food Science and*
613 *Technology* 48: 40–50.

614 Hong, Shu et al. 2018. “Versatile Acid Base Sustainable Solvent for Fast Extraction of Various
615 Molecular Weight Chitin from Lobster Shell.” *Carbohydrate Polymers* 201: 211–17.
616 <https://doi.org/10.1016/j.carbpol.2018.08.059>.

617 Huet, Gael et al. 2020. “Straightforward Extraction and Selective Bioconversion of High Purity Chitin
618 from Bombyx Eri Larva : Toward an Integrated Insect Biorefinery.” *Carbohydrate Polymers*
619 228: 115382. <https://doi.org/10.1016/j.carbpol.2019.115382>.

620 Husson, Eric et al. 2017. “Effect of Room Temperature Ionic Liquids on Selective Biocatalytic
621 Hydrolysis of Chitin via Sequential or Simultaneous Strategies.” *Green Chemistry* 19: 4122–31.
622 <http://pubs.rsc.org/en/Content/ArticleLanding/2017/GC/C7GC01471F>.

623 Iacob, Andreea Teodora et al. 2018. “Preparation, Characterization and Wound Healing Effects of
624 New Membranes Based on Chitosan, Hyaluronic Acid and Arginine Derivatives.” *Polymers*
625 8(6): 1–19.

626 Inukai, Yoshinari et al. 1998. “Selective Separation of Germanium(IV) by 2,3-Dihydroxypropyl
627 Chitosan Resin.” *Analytica Chimica Acta* 371: 187–93.

628 Khanafari, A, R Marandi, and Sh Sanathei. 2008. “Recovery of Chitin and Chitosan from Shrimp
629 Waste by Chemical and Microbial Methods.” *J. Environ. Health* 5: 19–24.

630 Lago, M. A. et al. 2011. “Compilation of Analytical Methods to Characterize and Determine Chitosan,
631 and Main Applications of the Polymer in Food Active Packaging.” *CYTA - Journal of Food* 9:
632 319–28.

633 Liu, Shaofang et al. 2012. “Extraction and Characterization of Chitin from the Beetle Holotrichia
634 Parallela Motschulsky.” *Molecules* 17: 4604–11.

635 Ma, Jia, and Yogeshwar Sahai. 2013. “Chitosan Biopolymer for Fuel Cell Applications.”
636 *Carbohydrate Polymers* 92: 955–75. <http://dx.doi.org/10.1016/j.carbpol.2012.10.015>.

637 Marroquin, Jason B., K. Y. Rhee, and S. J. Park. 2013. “Chitosan Nanocomposite Films: Enhanced
638 Electrical Conductivity, Thermal Stability, and Mechanical Properties.” *Carbohydrate Polymers*
639 92(2): 1783–91. <http://dx.doi.org/10.1016/j.carbpol.2012.11.042>.

640 Menzies, Kara L, and Lyndon Jones. 2010. “The Impact of Contact Angle on the Biocompatibility of
641 Biomaterials.” *Optometry and Vision Science* 87: 387–99.

642 Moussout, Hamou, Mustapha Aazza, and Hammou Ahlafi. 2020. *Chapter 5 : Thermal Degradation*
643 *Characteristics of Chitin, Chitosan, Al2O3/Chitosan, and Benonite/Chitosan Nanocomposites.*

644 Mukesh, Chandrakant, Dibyendu Mondal, Mukesh Sharma, and Kamalesh Prasad. 2014. “Choline
645 Chloride – Thiourea , a Deep Eutectic Solvent for the Production of Chitin Nanofibers.”
646 *Carbohydrate Polymers* 103: 466–71. <http://dx.doi.org/10.1016/j.carbpol.2013.12.082>.

647 Di Nardo, Thomas, Caroline Hadad, Albert Nguyen Van Nhien, and Audrey Moores. 2019. "Synthesis
648 of High Molecular Weight Chitosan from Chitin by Mechanochemistry and Aging." *Green*
649 *Chemistry* 21: 3276–85.

650 Niemczyk, A, A Kmiecik, M El Fray, and A Piegat. 2016. 21 Progress on Chemistry and Application
651 of Chitin and Its Derivatives *The Influence of C18-Fatty Acids on Chemical Structure of*
652 *Chitosan Derivatives and Their Thermal Properties*.

653 Niemczyk, Agata et al. 2019. "Biofunctional Catheter Coatings Based on Chitosan-Fatty Acids
654 Derivatives." *Carbohydrate Polymers* 225: 115263.

655 Niemczyk, Agata, Mirosława El Fray, and Steve E. Franklin. 2015. "Friction Behaviour of Hydrophilic
656 Lubricious Coatings for Medical Device Applications." *Tribology International* 89: 54–61.

657 Nogales-Mérida, Silvia et al. 2019. "Insect Meals in Fish Nutrition." *Reviews in Aquaculture* 11(4):
658 1080–1103.

659 Pan, Yan et al. 2002. "Bioadhesive Polysaccharide in Protein Delivery System.Pdf." *International*
660 *Journal of Pharmaceutics* 249: 139–47.

661 Ruggeri, S. et al. 2019. "Chemical and Electrochemical Properties of a Hydrophobic Deep Eutectic
662 Solvent." *Electrochimica Acta* 295: 124–29.

663 Shamshina, J. L. et al. 2016. "Pulping of Crustacean Waste Using Ionic Liquids: To Extract or Not to
664 Extract." *ACS Sustainable Chemistry and Engineering* 4: 6072–81.

665 Shamshina, Julia L. 2019. "Chitin in Ionic Liquids: Historical Insights into the Polymer's Dissolution
666 and Isolation. A Review." *Green Chemistry* 21: 3974–93.

667 Singh, Balvant Shyam, Hyacintha Rennet Lobo, and Ganapati Subray Shankarling. 2012. "Choline
668 Chloride Based Eutectic Solvents: Magical Catalytic System for Carbon-Carbon Bond Formation
669 in the Rapid Synthesis of β -Hydroxy Functionalized Derivatives." *Catalysis Communications* 24:
670 70–74. <http://dx.doi.org/10.1016/j.catcom.2012.03.021>.

671 Song, Chao et al. 2013. "Physicochemical Properties and Antioxidant Activity of Chitosan from the
672 Blowfly *Chrysomya Megacephala* Larvae." *International Journal of Biological Macromolecules*
673 60: 347–55.

674 Le Tien, Canh, Monique Lacroix, Pompilia Ispas-Szabo, and Mircea Alexandru Mateescu. 2003. "N-
675 Acylated Chitosan: Hydrophobic Matrices for Controlled Drug Release." *Journal of Controlled*
676 *Release* 93: 1–13.

677 Vicente, Filipa A., Bojana Bradić, Uroš Novak, and Blaž Likozar. 2020. " α -Chitin Dissolution, N-
678 Deacetylation and Valorization in Deep Eutectic Solvents." *Biopolymers* 111: 1–9.

679 Wang, Jianlong, and Can Chen. 2014. "Chitosan-Based Biosorbents: Modification and Application for
680 Biosorption of Heavy Metals and Radionuclides." *Bioresource Technology* 160: 129–41.

681 Wineinger, Hannah B. et al. 2020. "A Method for Determining the Uniquely High Molecular Weight
682 of Chitin Extracted from Raw Shrimp Shells Using Ionic Iquids." *Green Chemistry* 22(12):
683 3734–41.

684 Young-Hee, Lee et al. 2008. "Oxidative Stress Resistance through Blocking Hsp60 Translocation
685 Followed by SAPK/JNK Inhibition in Aged Human Diploid Fibroblast." *Cell biochemistry and*
686 *function* 26: 320–28.

687 Zdanowicz, Magdalena, Katarzyna Wilpiszewska, and Tadeusz Szychaj. 2018. "Deep Eutectic
688 Solvents for Polysaccharides Processing. A Review." *Carbohydrate Polymers* 200: 361–80.
689 <https://doi.org/10.1016/j.carbpol.2018.07.078>.

690 Zhao, Xinhui et al. 2018. "Deep Eutectic-Solvothermal Synthesis of Nanostructured Fe₃S₄ for
691 Electrochemical N₂ Fixation under Ambient Conditions." *Chemical Communications* 54: 13010–
692 13.

693 Zhu, Ping, Zhongji Gu, Shu Hong, and Hailan Lian. 2017. "One-Pot Production of Chitin with High
694 Purity from Lobster Shells Using Choline Chloride–Malonic Acid Deep Eutectic Solvent."
695 *Carbohydrate Polymers* 177: 217–23. <https://doi.org/10.1016/j.carbpol.2017.09.001>.

696 Ziegler-Borowska, Marta, Dorota Chełminiak, Halina Kaczmarek, and Anna Kaczmarek-Kędziera.
697 2016. "Effect of Side Substituents on Thermal Stability of the Modified Chitosan and Its
698 Nanocomposites with Magnetite." *Journal of Thermal Analysis and Calorimetry* 124(3): 1267–
699 80.

700